



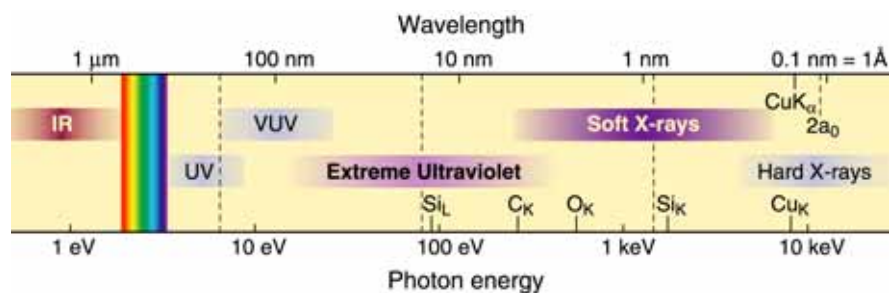
EUV and Soft X-Ray Optics

David Attwood
University of California, Berkeley

Cheiron School
September 2012
SPRING-8

CheironSchool_Sept2012_Lec1.ppt 1

The short wavelength region of the electromagnetic spectrum



- See smaller features
- Write smaller patterns
- Elemental and chemical sensitivity

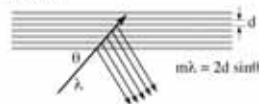
$$\hbar\omega \cdot \lambda = hc = 1239.842 \text{ eV nm}$$

$$n = 1 - \delta + i\beta \quad \delta, \beta \ll 1$$

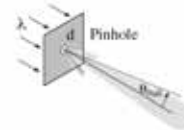
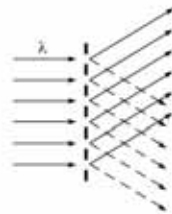
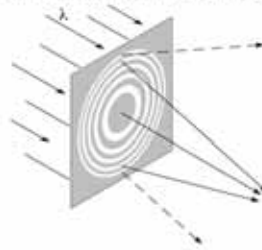
CheironSchool_Sept2012_Lec1.ppt 2

Available x-ray optical techniques

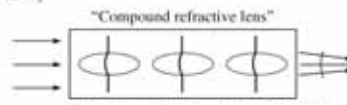
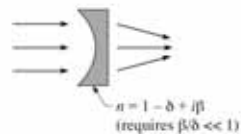
- Reflection (glancing incidence or multilayer coatings)



- Diffraction (zone plates, gratings, pinholes)



- Refraction (only for hard x-rays, > 20 keV)

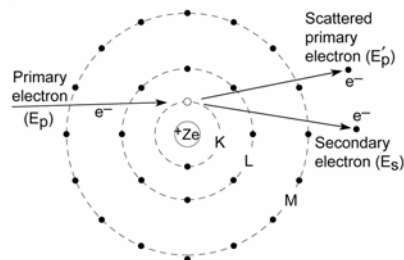


A. Snigirev et al., *Nature* 384, 49 (7 Nov. 1996)
B. Lengeler et al., *J. Appl. Phys.* 84, 5855 (1 Dec. 1998)

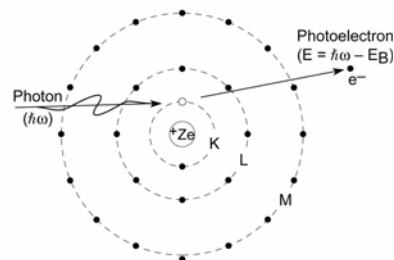
CheironSchool_Sept2012_Lec1.ppt 3

Basic ionization and emission processes in isolated atoms

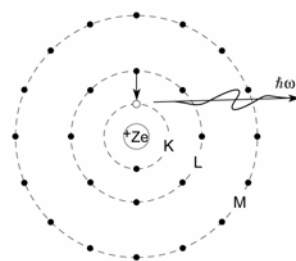
(a) Electron collision induced ionization



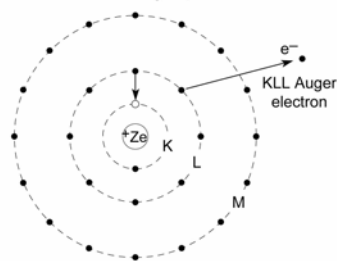
(b) Photoionization



(c) Fluorescent emission of characteristic radiation

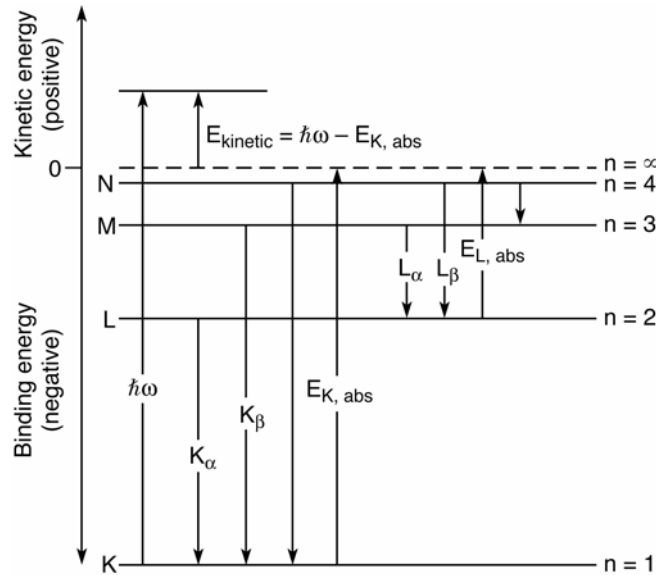


(d) Non-radiative Auger process



Ch01_F02VG.ai
CheironSchool_Sept2012_Lec1.ppt 4

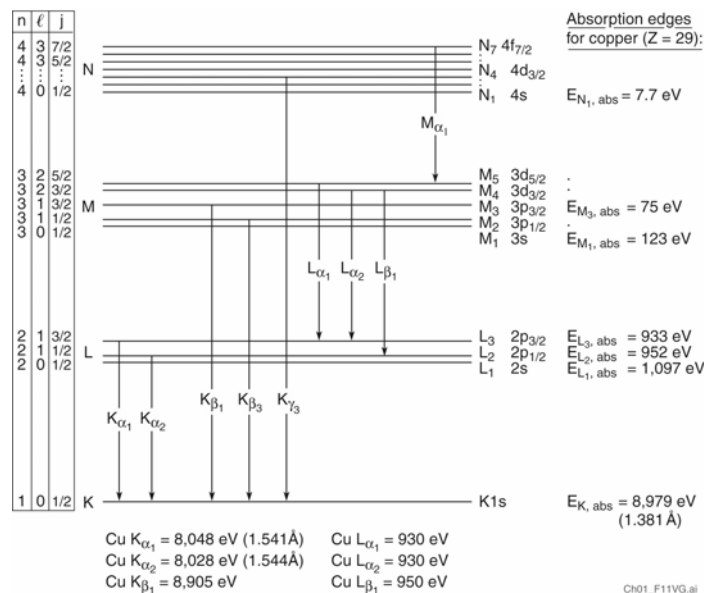
Energy levels, absorption edges, and characteristic line emissions for a multi-electron atom



Ch01_F10VG.ai

CheironSchool_Sept2012_Lec1.ppt 5

Energy levels, quantum numbers, and allowed transitions for the copper atom



Ch01_F11VG.ai

CheironSchool_Sept2012_Lec1.ppt 6

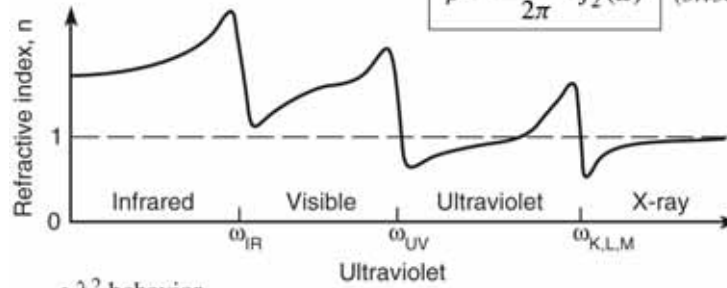
Refractive index from the IR to x-ray spectral region



$$n(\omega) = 1 - \delta + i\beta \quad (3.12)$$

$$\delta = \frac{n_a r_e \lambda^2}{2\pi} f_1^0(\omega) \quad (3.13a)$$

$$\beta = \frac{n_a r_e \lambda^2}{2\pi} f_2^0(\omega) \quad (3.13b)$$



- λ^2 behavior
- δ & $\beta \ll 1$
- δ -crossover

Ch03_RefrIndex01.XPS.ai

CheironSchool_Sept2012_Lec1.ppt 7

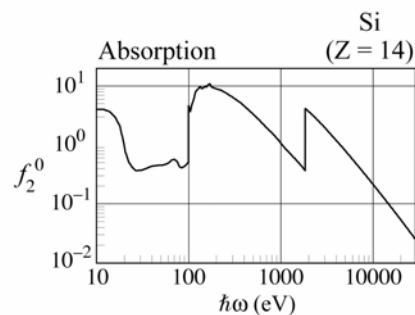
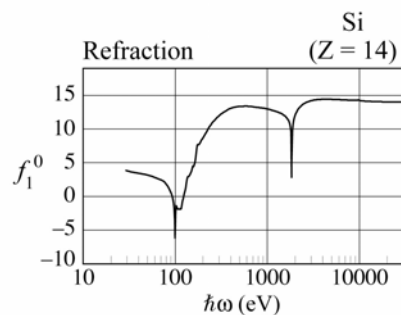
Refractive index at nanometer wavelengths



Refractive Index

$$n = 1 - \delta + i\beta = 1 - \frac{n_a r_e \lambda^2}{2\pi} (f_1^0 - if_2^0)$$

Atomic scattering factors



ScattmgRefrIndex_June2009.ai

CheironSchool_Sept2012_Lec1.ppt 8

Refractive index in the soft x-ray and EUV spectral region



$$n(\omega) = 1 - \frac{1}{2} \frac{e^2 n_a}{\epsilon_0 m} \sum_s \frac{g_s}{(\omega^2 - \omega_s^2) + i\gamma\omega} \quad (3.8)$$

Noting that

$$r_e = \frac{e^2}{4\pi\epsilon_0 mc^2}$$

and that for forward scattering

$$f^0(\omega) = \sum_s \frac{g_s \omega^2}{\omega^2 - \omega_s^2 + i\gamma\omega}$$

where this has complex components

$$f^0(\omega) = f_1^0(\omega) - if_2^0(\omega)$$

The refractive index can then be written as

$$n(\omega) = 1 - \frac{n_a r_e \lambda^2}{2\pi} [f_1^0(\omega) - if_2^0(\omega)] \quad (3.9)$$

which we write in the simplified form

$$n(\omega) = 1 - \delta + i\beta \quad (3.12)$$

Ch03_RefracIndex2.ai

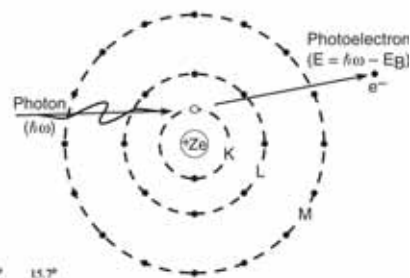
CheironSchool_Sept2012_Lec1.ppt 9

Photoionization and electron binding energies



TABLE B.1. Electron binding energies in electron volts for the elements in their natural forms.^a

Element	K Is	L ₁ 2s	L ₂ 2p _{1/2}	L ₃ 2p _{3/2}	M ₂ 3s	M ₃ 3p _{1/2}	M ₄ 3p _{3/2}	M ₅ 3d _{3/2}	M ₆ 3d _{5/2}	N ₁ 4s	N ₂ 4p _{1/2}	N ₃ 4p _{3/2}
1 H	13.6											
2 He	24.6 ^a											
3 Li	54.7 ^a											
4 Be	111.5 ^a											
5 B	188 ^a											
6 C	284.2 ^a											
7 N	409.9 ^a	37.3 ^a										
8 O	543.1 ^a	41.6 ^a										
9 F	696.7 ^a											
10 Ne	870.2 ^a	48.5 ^a	21.7 ^a	21.6 ^a								
11 Na	1070.8 ^a	63.5 ^a	30.4 ^a	30.5 ^a								
12 Mg	1303.0 ^a	88.0 ^a	49.6 ^a	49.2 ^a								
13 Al	1559.6	117.8 ^a	72.9 ^a	72.5 ^a								
14 Si	1838.9	149.7 ^a	99.8 ^a	99.2 ^a								
15 P	2143.5	189 ^a	139 ^a	135 ^a								
16 S	2472	230.9 ^a	163.6 ^a	162.5 ^a								
17 Cl	2822.4	270.2 ^a	202 ^a	200 ^a								
18 Ar	3205.9 ^a	326.3 ^a	250.6 ^a	248.4 ^a	29.3 ^a	15.9 ^a	15.7 ^a					
19 K	3608.4 ^a	378.6 ^a	297.3 ^a	294.6 ^a	34.8 ^a	18.3 ^a	18.3 ^a					
20 Ca	4038.5 ^a	438.4 ^a	349.7 ^a	346.2 ^a	44.3 ^a	25.4 ^a	25.4 ^a					
21 Sc	4492.8	498.0 ^a	403.6 ^a	398.7 ^a	51.1 ^a	28.3 ^a	28.3 ^a					
22 Ti	4966.4	560.9 ^a	461.2 ^a	453.8 ^a	58.7 ^a	32.6 ^a	32.6 ^a					
23 V	5465.1	626.7 ^a	519.8 ^a	512.1 ^a	66.3 ^a	37.2 ^a	37.2 ^a					
24 Cr	5989.2	695.7 ^a	583.8 ^a	574.1 ^a	74.1 ^a	42.2 ^a	42.2 ^a					
25 Mn	6539.0	769.1 ^a	649.9 ^a	638.7 ^a	82.3 ^a	47.2 ^a	47.2 ^a					
26 Fe	7112.0	844.6 ^a	719.9 ^a	706.8 ^a	91.3 ^a	52.7 ^a	52.7 ^a					
27 Co	7708.9	925.1 ^a	793.3 ^a	778.1 ^a	101.0 ^a	58.9 ^a	58.9 ^a					
28 Ni	8332.8	1008.6 ^a	870.0 ^a	852.7 ^a	110.8 ^a	66.0 ^a	66.2 ^a					
29 Cu	8978.9	1096.7 ^a	952.3 ^a	932.5 ^a	122.5 ^a	77.3 ^a	75.1 ^a					
30 Zn	9658.6	1196.2 ^a	1044.9 ^a	1021.8 ^a	139.8 ^a	91.4 ^a	88.6 ^a	10.2 ^a	10.1 ^a			

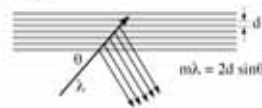
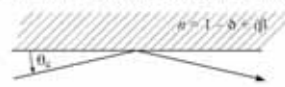


©2011 ARL, Inc.
B. Photoionization

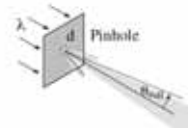
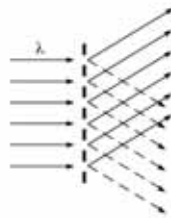
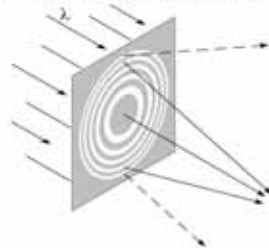
CheironSchool_Sept2012_Lec1.ppt 10

Available x-ray optical techniques

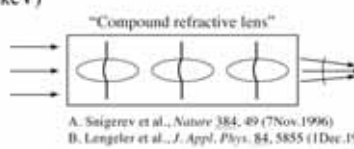
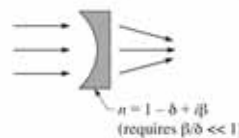
- Reflection (glancing incidence or multilayer coatings)



- Diffraction (zone plates, gratings, pinholes)



- Refraction (only for hard x-rays, > 20 keV)

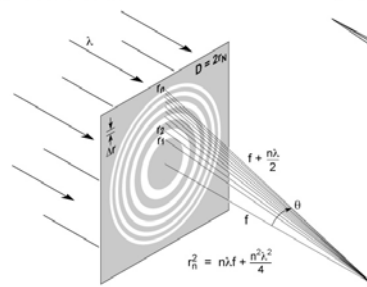


A. Snigirev et al., *Nature* 384, 49 (7 Nov. 1996)
B. Lengele et al., *J. Appl. Phys.* 84, 5855 (1 Dec. 1998)

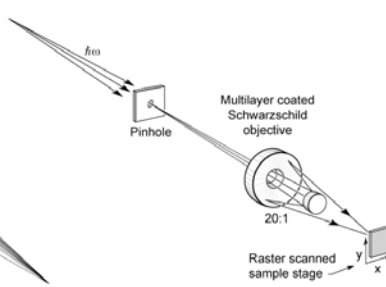
CheironSchool_Sept2012_Lec1.ppt 11

Diffraction and reflective optics for EUV, soft x-rays and hard x-rays

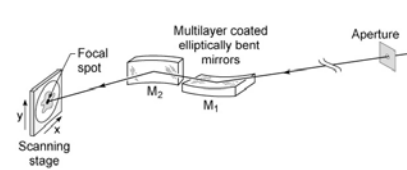
a) Fresnel zone plate



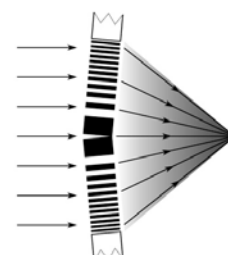
b) Schwarzschild objective



c) Kirkpatrick-Baez mirror pair

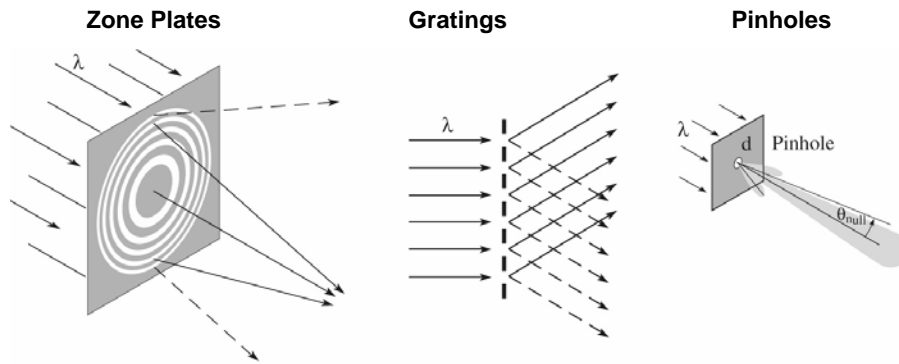


d) Multilayer Laue lens



CheironSchool_Sept2012_Lec1.ppt 12

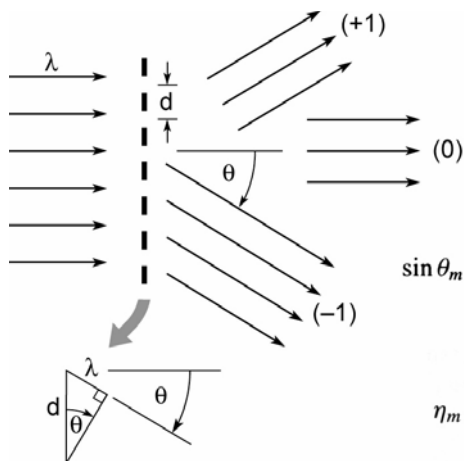
Diffractive optics for soft x-rays and EUV



DiffractionOptics.ai

CheironSchool_Sept2012_Lec1.ppt 13

Diffraction from a transmission grating



$$\sin \theta_m = \frac{m\lambda}{d}; \quad m = 0, \pm 1, \pm 2, \pm 3, \dots \quad (9.2)$$

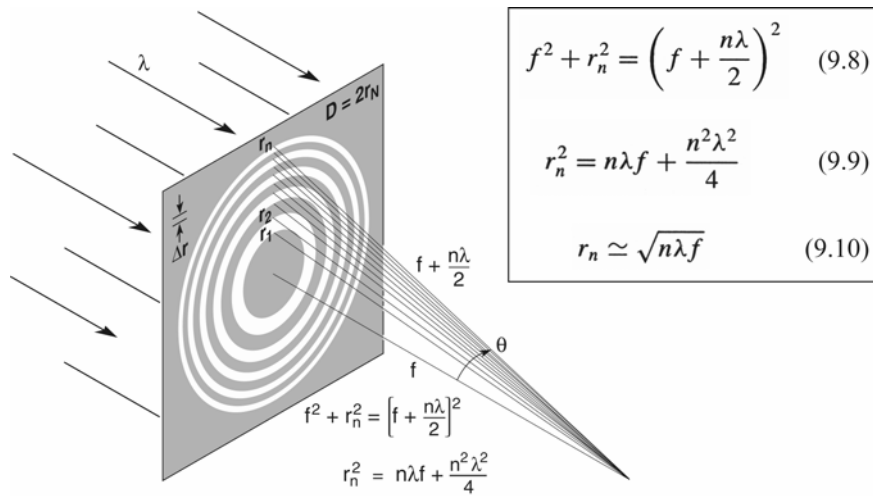
$$\eta_m = \begin{cases} \frac{1}{4} & m = 0 \\ 1/m^2\pi^2 & m \text{ odd} \\ 0 & m \text{ even} \end{cases} \quad (9.24)$$

(50% absorbed)

Ch09_F03VGrev.4.04.ai

CheironSchool_Sept2012_Lec1.ppt 14

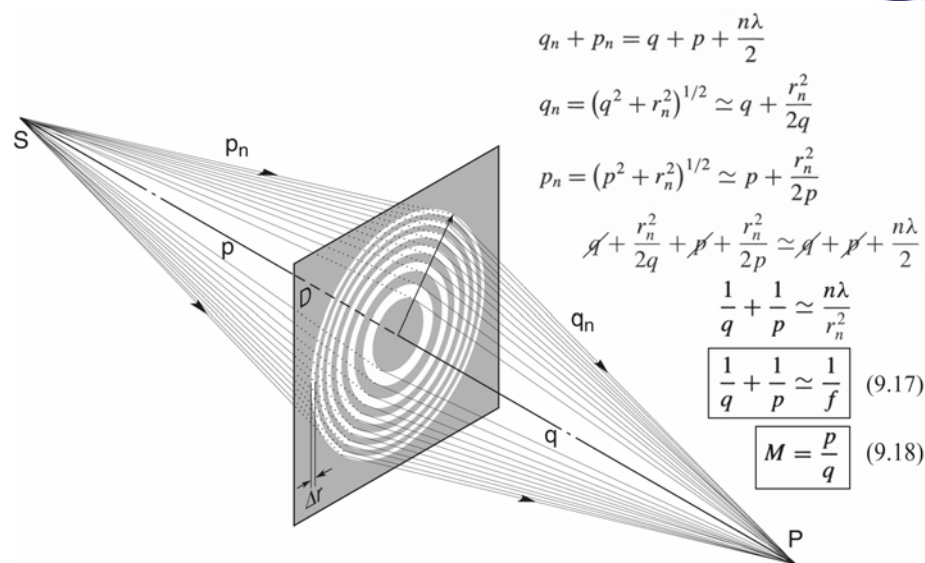
A Fresnel zone plate lens



Ch09_F05VG.ai

CheironSchool_Sept2012_Lec1.ppt 15

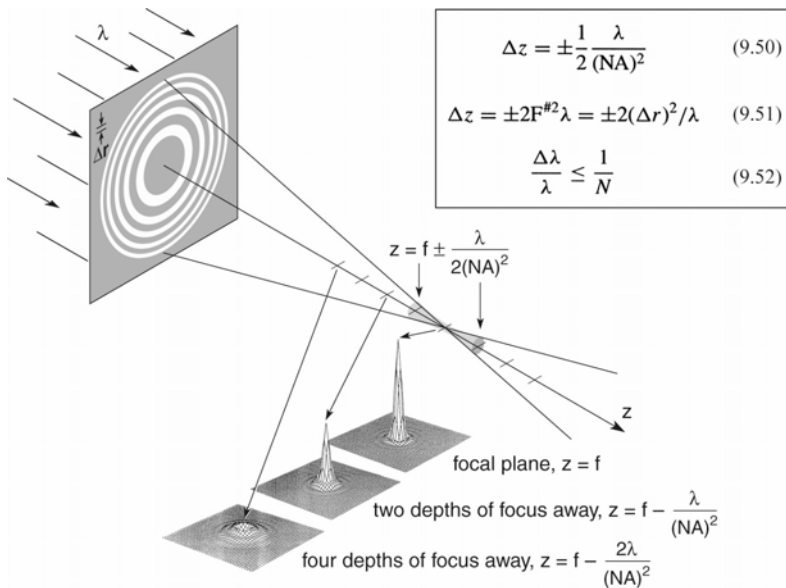
A Fresnel zone plate lens used as a diffractive lens for point to point imaging



Ch09_F02_modif.VG.ai

CheironSchool_Sept2012_Lec1.ppt 16

Depth of focus and spectral bandwidth



Ch09_F18_mod01.VG.ai

CheironSchool_Sept2012_Lec1.ppt 17




A Fresnel zone plate lens for soft x-ray microscopy




Courtesy of E. Anderson, LBNL

CheironSchool_Sept2012_Lec1.ppt 18

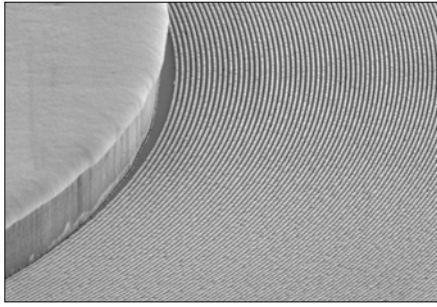


Zone plates for ALS STXM beamlines – “3D Engineered Nanostructures”

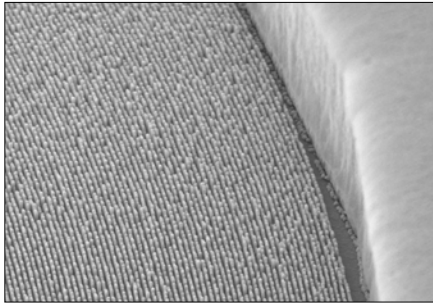


$\Delta r = 35 \text{ nm}$, $\Delta t = 180 \text{ nm Au}$, $N = 1700$
 $D = 240 \text{ }\mu\text{m}$, $3 \times 95 \text{ }\mu\text{m}^2$ central stop

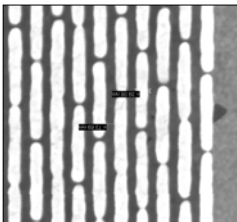
Inner zones




Outer zones




Outer zone close-up

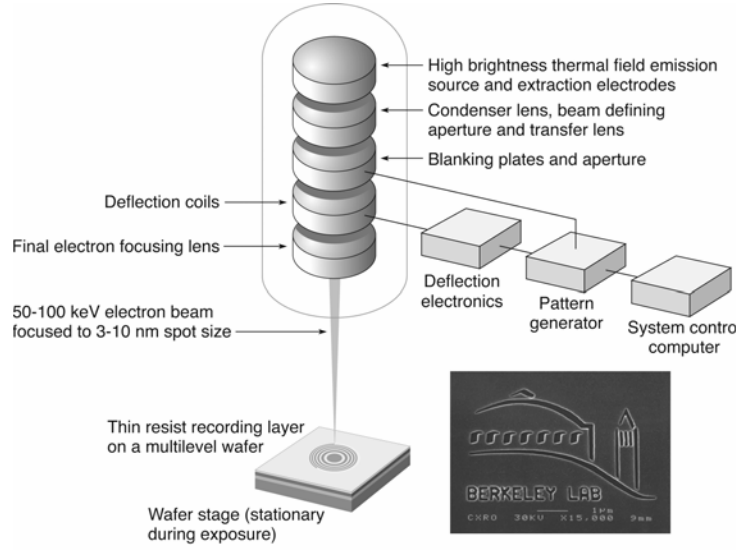


CheironSchool_Sep2012_Lec1.ppt 19



The Nanowriter: high resolution electron beam writing with high placement accuracy





Thin resist recording layer on a multilevel wafer

Wafer stage (stationary during exposure)

High brightness thermal field emission source and extraction electrodes

Condenser lens, beam defining aperture and transfer lens

Blanking plates and aperture

Deflection coils

Final electron focusing lens

50-100 keV electron beam focused to 3-10 nm spot size

Deflection electronics

Pattern generator

System control computer

Courtesy of E. Anderson (LBNL)

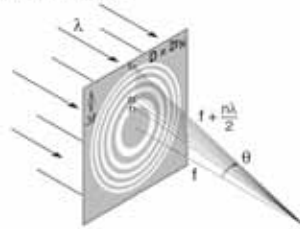
CH09_F43VG.ai

CheironSchool_Sep2012_Lec1.ppt 20

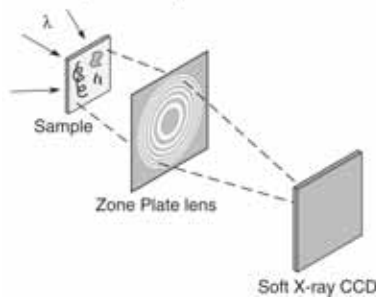
Zones plates for soft x-ray image formation



Zone Plate Lens



Soft X-Ray Microscope



Zone Plate Formulae

$$r_n^2 = n\lambda f + \frac{n^2\lambda^2}{4} \quad (9.9)$$

$$D = 4N\Delta r \quad (9.13)$$

$$f = \frac{4N(\Delta r)^2}{\lambda} \quad (9.14)$$

$$NA = \frac{\lambda}{2\Delta r} \quad (9.15)$$

$$\text{Res.} = k_1 \frac{\lambda}{NA} = 2k_1 \Delta r \quad \begin{cases} k_1 = 0.61 \\ (\sigma = 0) \end{cases} \quad \begin{cases} 1.22\Delta r = 30 \text{ nm} \\ k_1 = 0.4 \\ (\sigma = 0.45) \end{cases} \quad \begin{cases} 0.8\Delta r = 19 \text{ nm} \end{cases}$$

$$\text{DOF} = \pm \frac{1}{2} \frac{\lambda}{(NA)^2} \quad (9.50)$$

$$\frac{\Delta\lambda}{\lambda} \leq \frac{1}{N} \quad (9.52)$$

$\lambda = 2.5 \text{ nm}$,
 $\Delta r = 25 \text{ nm}$
 $N = 618$

$63 \mu\text{m}$

0.63 mm

0.05

$1.22\Delta r = 30 \text{ nm}$

$0.8\Delta r = 19 \text{ nm}$

$1 \mu\text{m}$

$1/700$

CheironSchool_Sept2012_Lec1.ppt 21

New x-ray lenses: Improving contrast and resolution for x-ray microscopy



C. Chang, A. Sakdinawat, P.J. Fischer, E.H. Anderson, D.T. Attwood, Opt. Lett. 2006; Sakdinawat and Liu, Opt. Lett. 2007; Sakdinawat and Liu, Opt. Express 2008

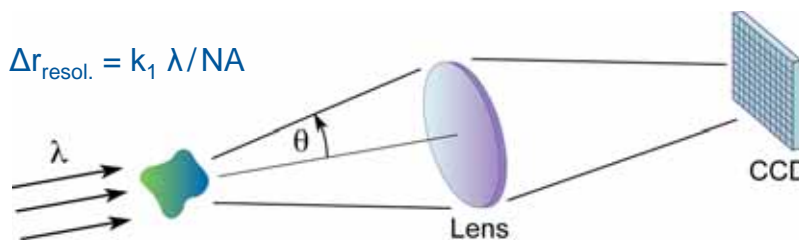
CheironSchool_Sept2012_Lec1.ppt 22

Diffraction limited x-ray imaging



Diffraction limited imaging is limited by the finite wavelength and acceptance aperture:

$$\Delta r_{\text{resol.}} = k_1 \lambda / \text{NA}$$



where $\text{NA} = n \sin \theta$ and the constant k_1 depends on illumination and specific image modulation criteria.

For x-rays

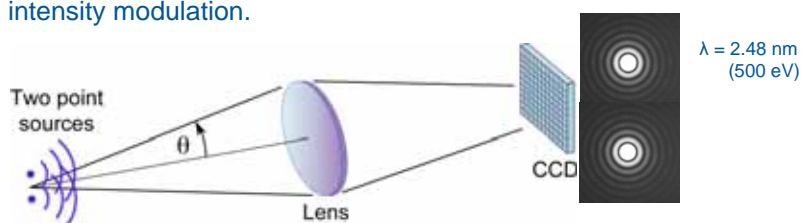
$$n = 1 - \delta + i\beta \quad \delta, \beta \ll 1$$

CheironSchool_Sept2012_Lec1.ppt 23

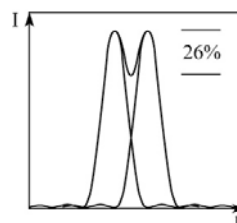
Diffraction limited x-ray imaging



For example, the widely accepted Rayleigh criteria for resolving two adjacent, mutually incoherent, point sources of light, results in a 26% intensity modulation.



Two overlapping Airy patterns



$$\Delta r_{\text{resol.}} = 0.61 \lambda / \text{NA}$$

Note: Other definitions are possible, depending on the application and the ability to discern separated objects.

Resultant intensity pattern when the two point sources are "just resolved", such that the central lobe maximum due to one point source overlaps the first minimum (dark ring) of the other.

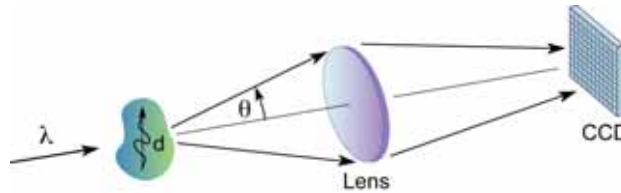
CheironSchool_Sept2012_Lec1.ppt 24

Resolution and illumination

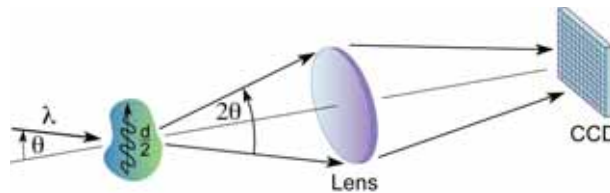


Achievable resolution can be improved by varying illumination:

An object pattern of periodicity d diffracts light and is just captured by the lens – setting the diffraction limited resolution limit.

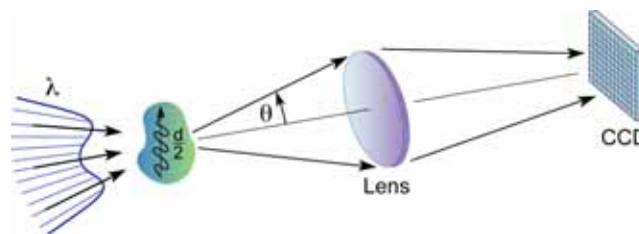


Diffraction from an object of smaller periodicity, $d/2$, is just captured, and resolved, when illuminated from an angle.

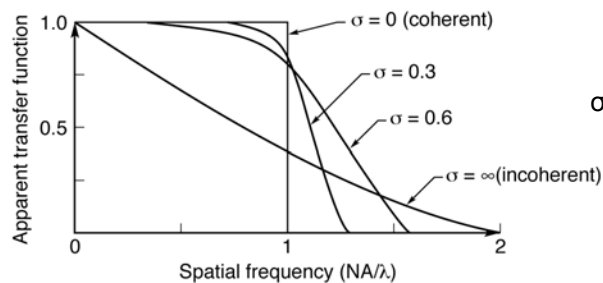


CheironSchool_Sept2012_Lec1.ppt 25

Resolution, illumination, and optical transfer function




Spatial frequency response of the optical system can be optimized by tailoring the angular distribution of illumination.




$$\sigma = \frac{NA_{\text{cond}}}{NA_{\text{obj}}} \quad (10.3)$$

CheironSchool_Sept2012_Lec1.ppt 26



Nature

LETTERS



Vol 435/30 June 2005/doi:10.1038/nature-3719

Soft X-ray microscopy at a spatial resolution better than 15 nm

Weilun Chao^{1,2}, Bruce D. Harteneck¹, J. Alexander Liddle¹, Erik H. Anderson¹ & David T. Attwood^{1,2}

Analysing tools that have spatial resolution at the nanometre scale are indispensable for the life and physical sciences. It is desirable that these tools also permit elemental and chemical identification on a scale of 10 nm or less, with large penetration depths. A variety of techniques^{1–3} in X-ray imaging are currently being developed that may provide these combined capabilities. Here we report the achievement of sub-15-nm spatial resolution with a soft X-ray microscope—and a clear path to below 10 nm—using an overlay technique for zone plate fabrication. The microscope covers a spectral range from a photon energy of 200 eV (5 nm wavelength) to 1.8 keV (0.7 nm), so that primary K and L atomic resonances of elements such as C, N, O, Al, Ti, Fe, Cu and Ni can be probed. This X-ray microscopy technique is therefore suitable for a wide range of studies: biological imaging in the water window^{4,5}; studies of wet environmental samples^{6,7}; studies of magnetic nanostructures with both elemental and spin-orbit sensitivity^{8,9}; studies that require viewing through thin windows, coatings or substrates (such as buried electronic devices in a silicon chip¹⁰); and three-dimensional imaging of cryogenically fixed biological cells¹¹.

The microscope XM-1 at the Advanced Light Source (ALS) in Berkeley¹² is schematically shown in Fig. 1. The microscope type is similar to that pioneered by the Göttingen/BESSY group (ref. 13, and references therein). A ‘micro’ zone plate (MZP) projects a full-field image to an X-ray sensitive CCD (charge-coupled device), typically in one or a few seconds, often with several hundred images per day. The field-of-view is typically 10 µm, corresponding to a magnification of 2,500. The condenser zone plate (CZP), with a central stop, serves two purposes in that it provides partially coherent hollow-cone illumination¹⁴, and, in combination with a pinhole, serves as the

monochromator. Monochromatic radiation of $\lambda/\Delta\lambda = 500$ is used. Both zone plates are fabricated in-house, using electron beam lithography¹⁵.

The spatial resolution of a zone plate based microscope is equal to $1.22\lambda NA_{MZP}$, where λ is the wavelength, NA_{MZP} is the numerical aperture of the MZP, and I_0 is an illumination dependent constant, which ranges from 0.5 to 0.61. For a zone plate lens used at high magnification, $NA_{MZP} = \lambda/2\Delta r_{MZP}$, where Δr_{MZP} is the outermost (smallest) zone width of the MZP¹⁶. For the partially coherent illumination^{17,18} used here, $I_0 = 0.4$ and thus the theoretical resolution is $0.8\lambda NA_{MZP}$, as calculated using the SPLAT computer program¹⁹ (a two-dimensional scalar diffraction code, which evaluates partially coherent imaging). In previous results with a $\Delta r_{MZP} = 25$ nm zone plate, we reported²⁰ an unambiguous spatial resolution of 20 nm. Here we describe the use of an overlay nanofabrication technique that allows us to fabricate zone plates with finer outer zone widths, to $\Delta r_{MZP} = 15$ nm, and to achieve a spatial resolution of below 15 nm, with clear potential for further extension.

This technique overcomes nanofabrication limits due to electron beam broadening in high feature density patterning. Beam broadening results from electron scattering within the recording medium (resist), leading to a loss of image contrast and thus resolvability for

$\lambda = 1.52$ nm (815 eV)
 $\Delta r = 15$ nm
 $N = 500$
 $D = 30$ µm
 $f = 300$ µm
 $\sigma = 0.38$
 $0.8 \Delta r = 12$ nm

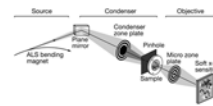
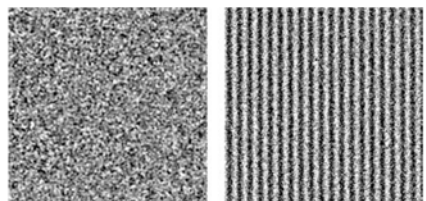



Figure 1 | A diagram of the soft X-ray microscope XM-1. The microscope uses a micro zone plate to project a full-field image onto a CCD camera that is sensitive to soft X-rays. Partially coherent, hollow-cone illumination of the sample is provided by a condenser zone plate. A central stop and a pinhole provide source illumination.

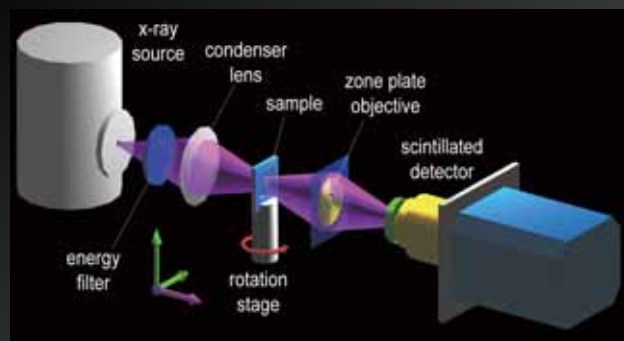
Figure 4 | Soft X-ray images of a 15.1 nm half-period test object, as formed with zone plates having outer zone widths of 25 nm and 15 nm.

Source: Weir, G. et al. Nature Photonics 1, 405–410 (2007). Department of Electrical Engineering, University of California, Berkeley, California 94720, USA.

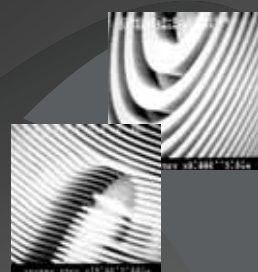
Hard x-ray zone plate microscopy

- Shorter wavelengths, potentially better spatial resolution and greater depth-of-field.
- Less absorption (β); phase shift (δ) dominates, higher efficiency.
- Thicker structures required (e.g., zones), higher aspect ratios pose nanofabrication challenges.
- Contrast of nanoscale samples minimal; will require good statistics, uniform background, dose mitigation.

Nanoscale hard x-ray tomography



X-ray Zone-plate Lens



Challenges for achieving nm scale resolution:

- High resolution objective lens: limiting the ultimate resolution
- High numerical aperture condenser lens:
- Detector: high efficiency for lab. source and high speed for synchrotron sources
- Precision mechanical system

Courtesy of Wenbing Yun and Michael Feser, Xradia

29

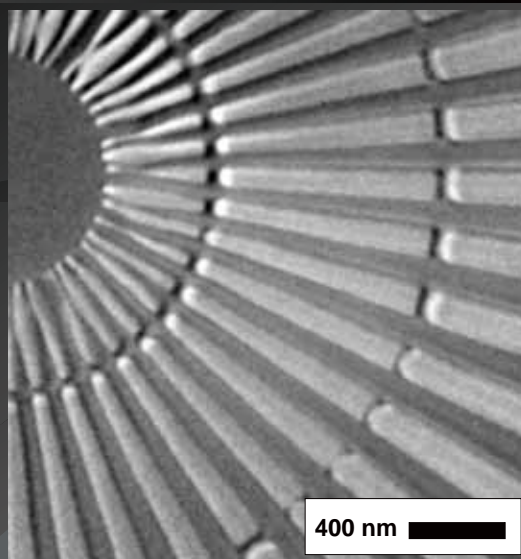
Xradia nanoXCT: Sub-25 nm Hard X-ray Image

Xradia Resolution Pattern

- 50 nm bar width
- 150 nm thick Au
- 8keV x-ray energy
- 3rd diffraction order

F. Duewer, M. Tang,
G. C. Yin, W. Yun,
M. Feser, et al.

Xradia nano-XCT
8-50S installed at
NSRRC, Taiwan

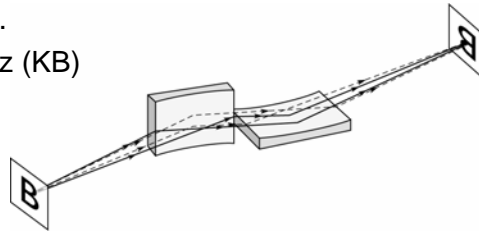


30

Hard x-ray imaging based on glancing incidence reflective optics

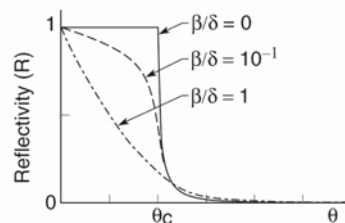
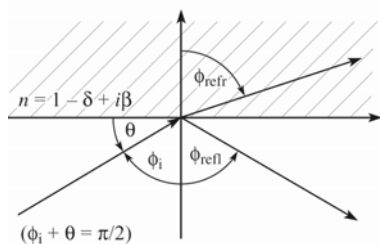


- Optics behave differently at these very short wavelengths (nanometers rather than 520 nm green light)
- The refractive index is less than unity, $n = 1 - \delta + i\beta$
- Waves bend away from the normal at an interface
- Absorption is significant in all materials and at all wavelength.
- Because of absorption, refractive lenses do not work, prisms do not, windows need to be extremely thin (100 nm or less).
- Because light is bent away from the surface normal, it possible to have “total external reflection” at glancing incidence – a commonly used technique.
- Kirkpatrick-Baez (KB) mirror pair



CheironSchool_Sept2012_Lec1.ppt 31

Glancing incidence optics



Snell's Law: $\sin \phi_{\text{refr.}} = \frac{\sin \phi_i}{n}$

Total external Reflection:

$$\phi_{\text{refr.}} \rightarrow \frac{\pi}{2} \text{ as } \phi_i \rightarrow \phi_{\text{critical}}$$

$$\text{Snell's Law: } 1 = \frac{\sin \phi_c}{1 - \delta}$$

$$\sin(90^\circ - \theta_c) = 1 - \delta$$

$$\cos \theta_c = 1 - \delta$$

$$1 - \frac{\theta_c^2}{2} = 1 - \delta$$

$$\theta_c = \sqrt{2\delta}$$

For gold at 1 keV

$$\delta = 2.1 \times 10^{-3}$$

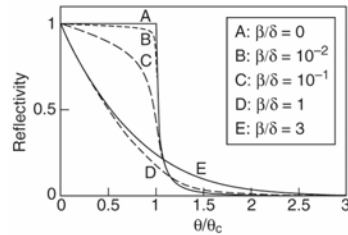
$$\theta_c = 3.7^\circ$$

(www.cxro.LBL.gov ;
“X-ray properties of the elements”
“X-ray interaction with matter”)

GlancingIncidenceOptics.ai
CheironSchool_Sept2012_Lec1.ppt 32

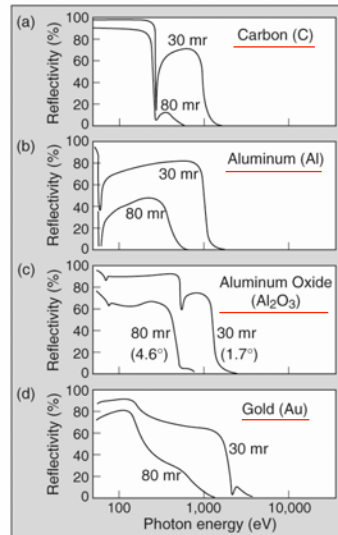
Total external reflection with finite β

Glancing incidence reflection
as a function of β/δ



- finite β/δ rounds the sharp angular dependence
- cutoff angle and absorption edges can enhance the sharpness
- note the effects of oxide layers and surface contamination

... for real materials



(Henke, Gullikson, Davis)

Ch03_TotalExtndReflec3.ai

CheironSchool_Sept2012_Lec1.ppt 33

Normal incidence reflection at an interface

$$R_s = \frac{|\cos \phi - \sqrt{n^2 - \sin^2 \phi}|^2}{|\cos \phi + \sqrt{n^2 - \sin^2 \phi}|^2} \quad (3.49)$$

at $\phi = 0$:

$$R_{s,\perp} = \frac{|1 - n|^2}{|1 + n|^2} = \frac{(1 - n)(1 - n^*)}{(1 + n)(1 + n^*)}$$

For $n = 1 - \delta + i\beta$

$$R_{s,\perp} = \frac{(\delta - i\beta)(\delta + i\beta)}{(2 - \delta + i\beta)(2 - \delta - i\beta)} = \frac{\delta^2 + \beta^2}{(2 - \delta)^2 + \beta^2}$$

Reflectivity for x-ray and EUV
radiation at normal incidence ($\phi = 0$):

$$R_{s,\perp} \simeq \frac{\delta^2 + \beta^2}{4} \quad (3.50)$$

Example: Nickel @ 300 eV (4.13 nm)

$$\left. \begin{array}{ll} f_1^o = 17.8 & f_2^o = 7.70 \\ \delta = 0.0124 & \beta = 0.00538 \end{array} \right\} R_{\perp} = 4.58 \times 10^{-5}$$

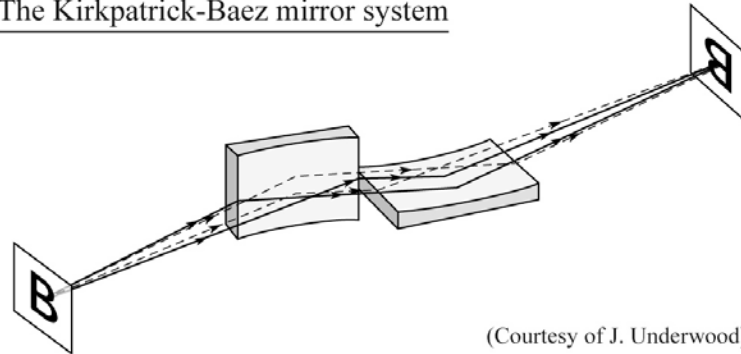
Ch03_NormIncldReflec_5.05.ai

CheironSchool_Sept2012_Lec1.ppt 34

Focusing with curved glancing incidence optics



The Kirkpatrick-Baez mirror system



(Courtesy of J. Underwood)

- Two crossed cylinders (or ellipses)
- Astigmatism cancels
- Common use in synchrotron radiation beamlines
- Hard x-ray microprobe

Ch03_FocusCurv_Sep2010.a

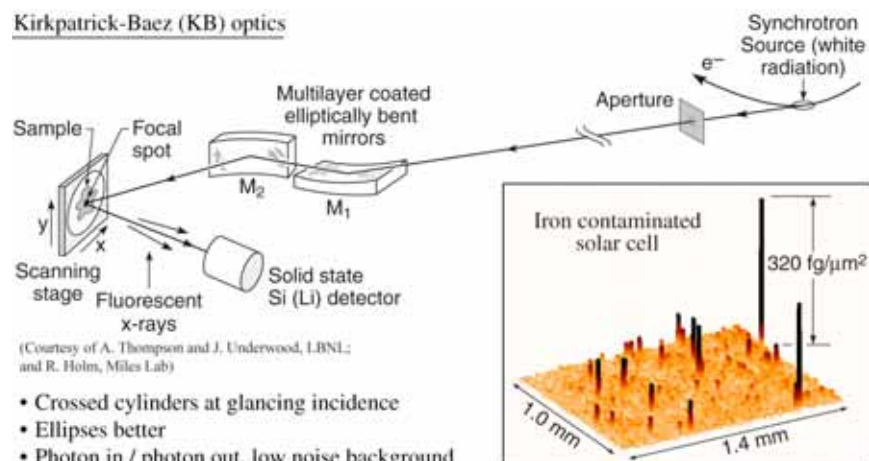
CheironSchool_Sep2012_Lec1.ppt 35



Fluorescent microprobe based in crossed cylinders



Kirkpatrick-Baez (KB) optics

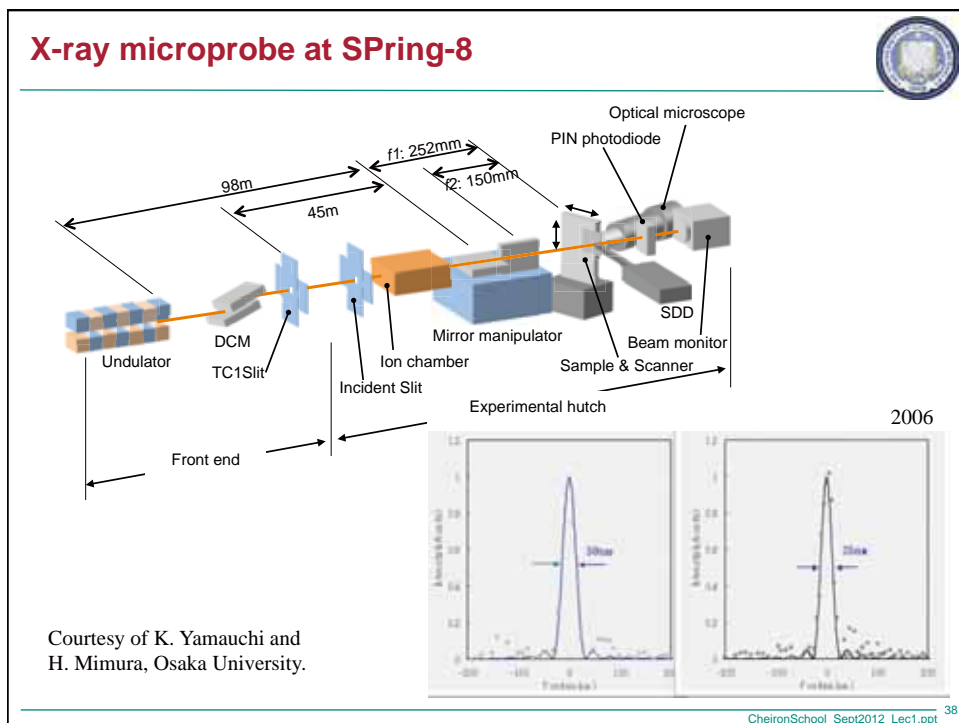
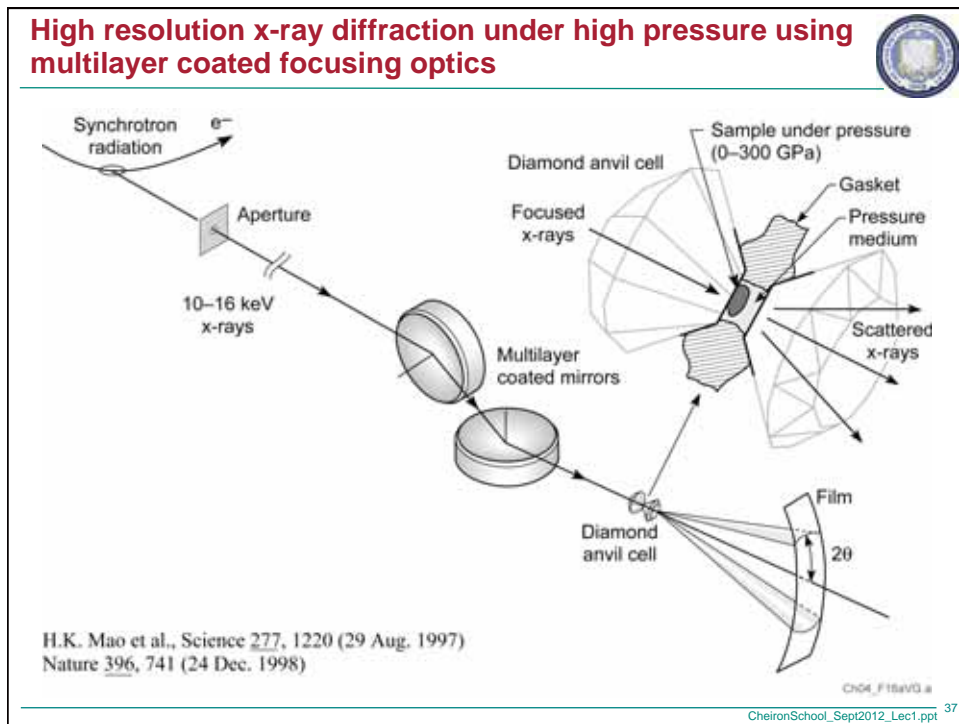


(Courtesy of A. Thompson and J. Underwood, LBNL;
and R. Holm, Miles Lab)

- Crossed cylinders at glancing incidence
- Ellipses better
- Photon in / photon out, low noise background
- Femtogram and part per billion (ppb) sensitivity
- Sub-micron focus (to $0.1 \mu\text{m}$ recently), but scattering gives several micron "50% encircled energy"
- K-B optics have many applications to synchrotron beamlines, fusion diagnostics, etc.

FluorescentMicroprobe.a

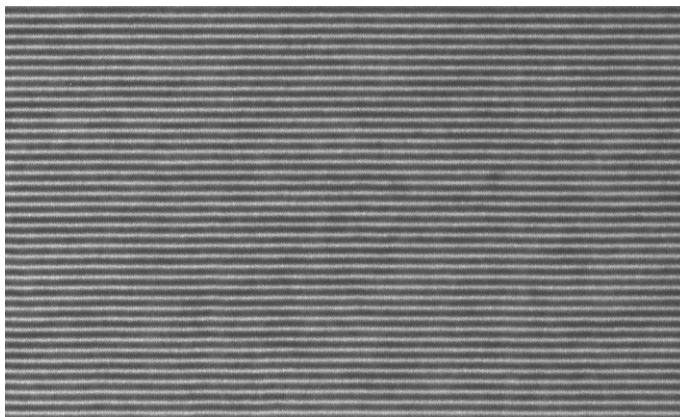
CheironSchool_Sep2012_Lec1.ppt 36



A high quality Mo/Si multilayer mirror



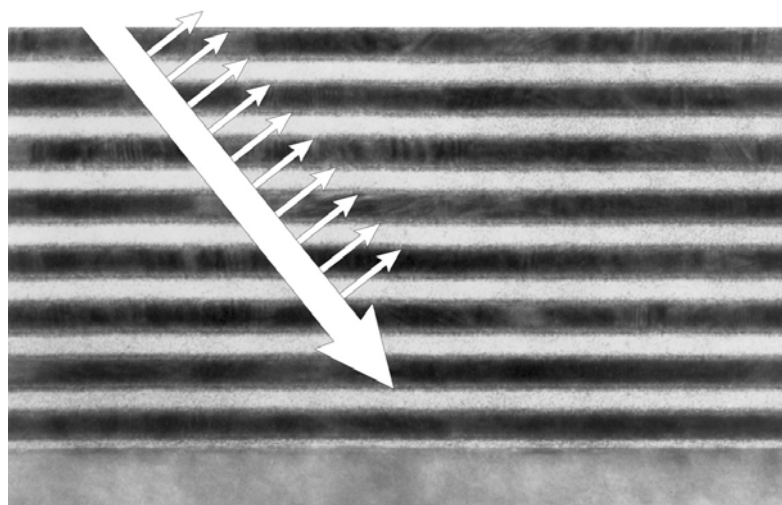
$N = 40$
 $d = 6.7$



Courtesy of Saša Bajt (LLNL)

CheironSchool_Sept2012_Lec1.ppt 39

Scattering by density variations within a multilayer coating



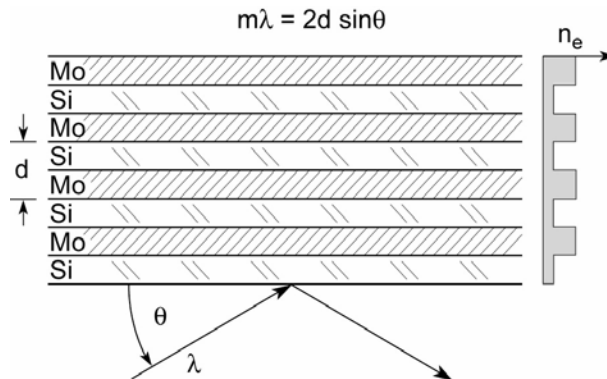
Mo/Si

(T. Nguyen, CXRO/LBNL)

Ch04_F01_Feb2007.ai

CheironSchool_Sept2012_Lec1.ppt 40

Multilayer mirrors satisfy the Bragg condition

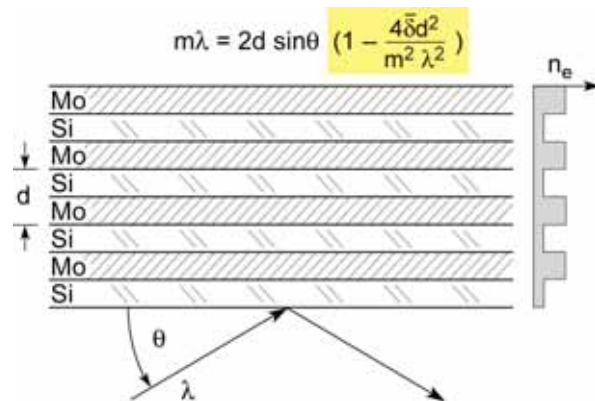


For normal incidence, $\theta = \pi/2$, first order ($m = 1$) reflection
 $\lambda = 2d$
 $d = \lambda/2$
 if the two layers are approximately equal
 $\Delta t \approx \lambda/4$
 a quarter-wave plate coating.

Ch04_MultilayerBragg01.ai

CheironSchool_Sept2012_Lec1.ppt 41

Multilayer mirrors satisfy the Bragg condition

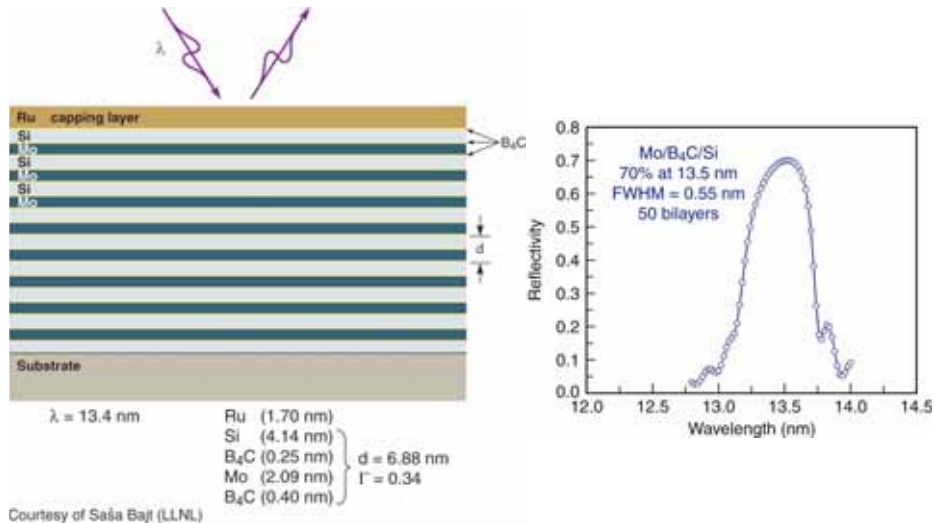


For normal incidence, $\theta = \pi/2$, first order ($m = 1$) reflection
 $\lambda = 2d$
 $d = \lambda/2$
 if the two layers are approximately equal
 $\Delta t = \lambda/4$
 a quarter-wave plate coating.

Ch04_MultilayerBragg02.ai

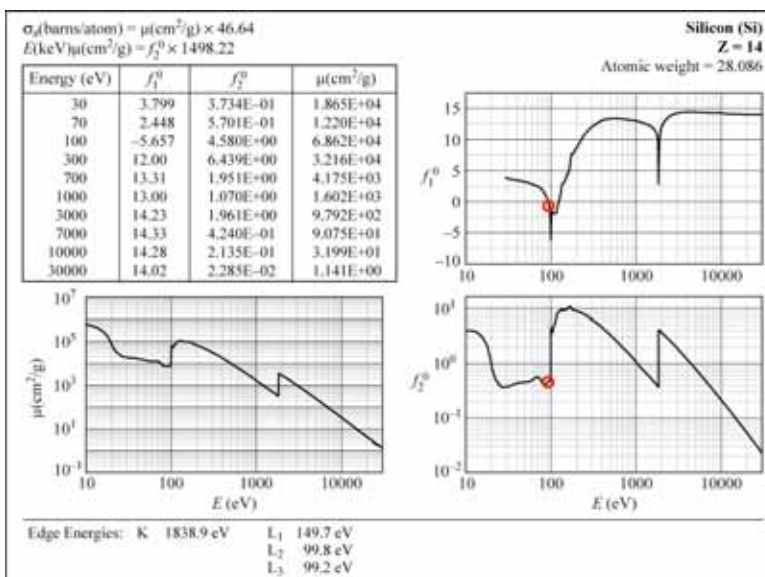
CheironSchool_Sept2012_Lec1.ppt 42

High reflectivity, thermally and environmentally robust multilayer coatings for high throughput EUV lithography



CheironSchool_Sept2012_Lec1.ppt 43

Atomic scattering factors for silicon (Z = 14)

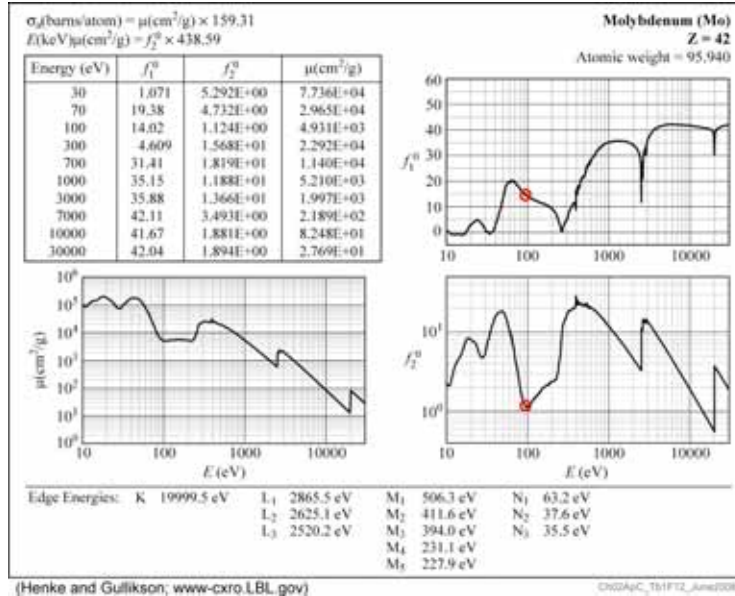


(Henke and Gullikson; www.cxro.lbl.gov)

ChOIAPic_Ts1PPT_Sept08.ai

CheironSchool_Sept2012_Lec1.ppt 44

Atomic scattering factors for molybdenum (Z = 42)



CheironSchool_Sept2012_Lec1.ppt 45

CXRO Web Site



X-Ray Interactions with Matter · Search CXRO

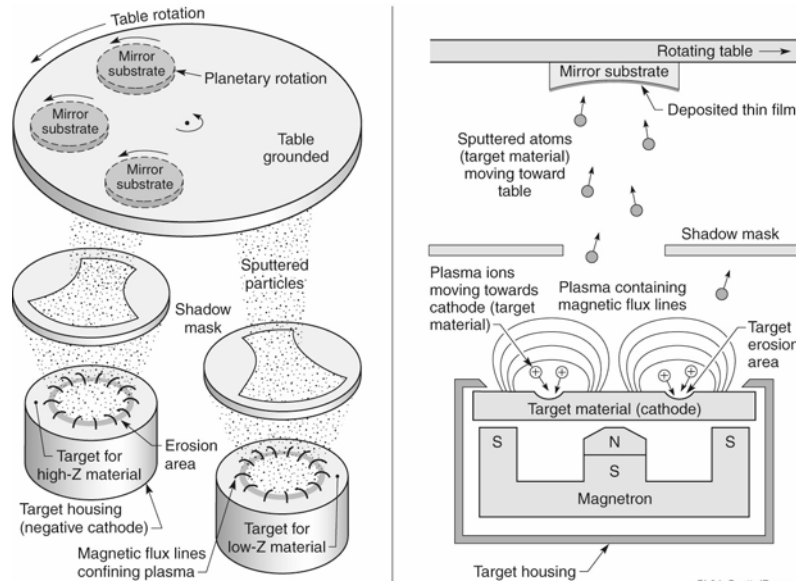
www.cxro.lbl.gov/

- Atomic scattering factors
- EUV/x-ray properties of the elements
- Index of refraction for compound materials
- Absorption, attenuation lengths, transmission
- EUV/x-ray reflectivity (mirrors, thin films, multilayers)
- Transmission grating efficiencies
- Multilayer mirror achievements
- Other

Facilities
Publications
Research
X-Ray Tools
Visitors
Personnel
Comments?
Server Stats

CheironSchool_Sept2012_Lec1.ppt 46

Sputtered deposition of a multilayer coating



Ch04_SputterDepo.ai
CheironSchool_Sept2012_Lec1.ppt 47



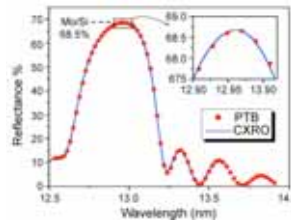
Multilayer coatings – “1D nanostructures”



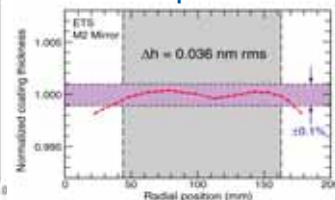
Eric Gullikson, Farhad Salmassi,
Yanwei Liu, Andy Aquila (grad),
Franklin Dollar (UG)



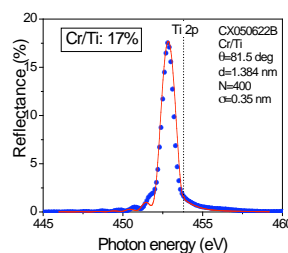
World reference standard



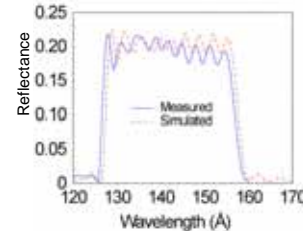
Creating uniformity for $\lambda/50$ optics



World record in water window



Wide band, narrow band, and chirped mirrors for fsec applications

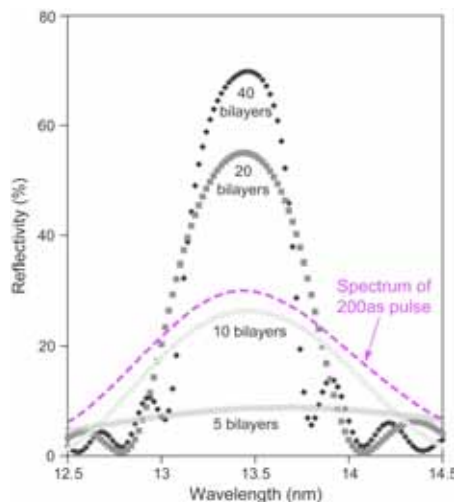


CheironSchool_Sept2012_Lec1.ppt 48

Broad bandwidth mirrors needed for as/fs pulses



$$\Delta E(\text{eV}) \cdot \Delta \tau(\text{fs}) \geq 1.8 \text{ fs} \cdot \text{eV (FWHM)}$$



- Multilayer mirrors depend on constructive interference from individual interfaces
- Higher reflectivity needs more layers
- Bandwidth gets narrower with more layers

Attosecond pulse

- Broad bandwidth
- Limited number of layers

N<10 layers required for 200 as pulse (@13nm)

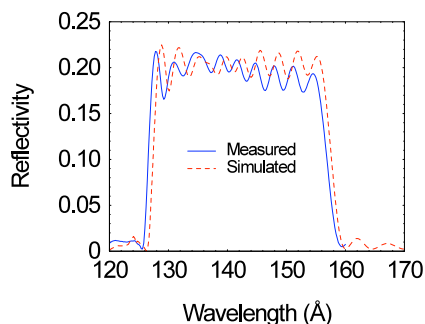
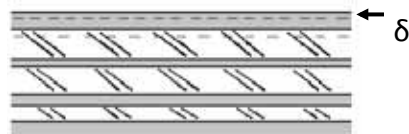
CheironSchool_Sept2012_Lec1.ppt 49



Aperiodic multilayers for asec application



Optimizing multilayers for specific applications requires the use of simulation of a multilayer stack with variations in the thickness of each material in the multilayer.



Successful design of aperiodic multilayers requires:

1. EM wave in multilayer structure
2. Optimization Algorithm
3. Sample preparation
4. Verification

A. L. Aquila, F. Salmassi, F. Dollar, Y. Liu, and E. Gullikson, "Developments in realistic design for aperiodic Mo/Si multilayer mirrors," *Opt. Express* **14**, 10073-10078 (2006)

CheironSchool_Sept2012_Lec1.ppt 50

The Cassegrain Telescope with multilayer coatings for EUV imaging of the solar corona

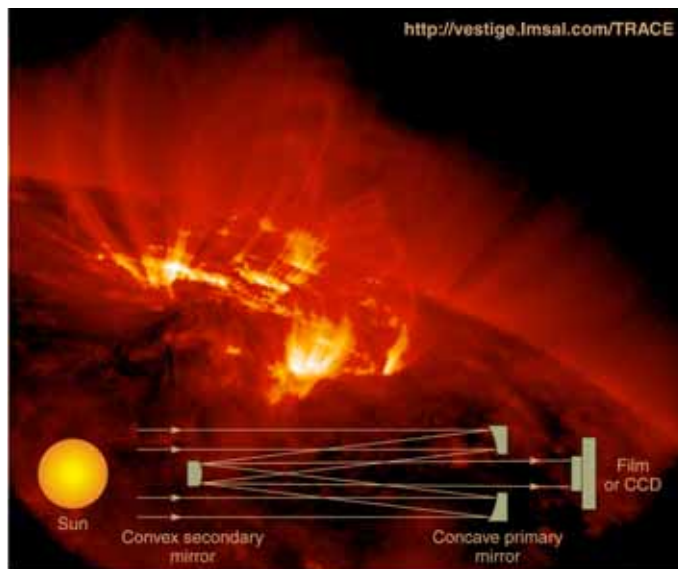
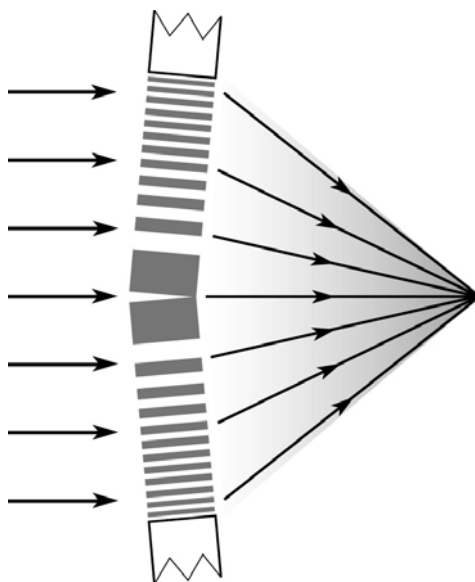


(Photo courtesy of L. Golub, Harvard-Smithsonian and T. Barbee, LLNL)

CheironSchool_Sept2012_Lec1.ppt 51

Multilayer Laue Lens for focusing hard x-rays



CheironSchool_Sept2012_Lec1.ppt 52

Photon energy, wavelength, power



$$\hbar\omega \cdot \lambda = hc = 1239.842 \text{ eV nm} \quad (1.1)$$

$$1 \text{ joule} \Rightarrow 5.034 \times 10^{15} \lambda[\text{nm}] \text{ photons} \quad (1.2a)$$

$$1 \text{ watt} \Rightarrow 5.034 \times 10^{15} \lambda[\text{nm}] \frac{\text{photons}}{\text{s}} \quad (1.2b)$$

Ch01_Eqs1.1_2.ai

CheironSchool_Sept2012_Lec1.ppt 53

Lectures online at www.youtube.com



Amazon.com



UC Berkeley

www.coe.berkeley.edu/AST/sxreuv

www.coe.berkeley.edu/AST/srms

www.coe.berkeley.edu/AST/sxr2009

CheironSchool_Sept2012_Lec1.ppt 54